

**A peer-reviewed version of this preprint was published in PeerJ on 30 September 2014.**

[View the peer-reviewed version](https://peerj.com/articles/597) (peerj.com/articles/597), which is the preferred citable publication unless you specifically need to cite this preprint.

Polka JK, Silver PA. 2014. Induced sensitivity of *Bacillus subtilis* colony morphology to mechanical media compression. PeerJ 2:e597  
<https://doi.org/10.7717/peerj.597>

1 Induced sensitivity of *Bacillus subtilis* colony morphology to mechanical  
2 media compression  
3

4 Jessica K. Polka<sup>1,2</sup> and Pamela A. Silver<sup>1,2</sup> \*

5  
6 1. Systems Biology Department, Harvard Medical School

7 2. Wyss Institute for Biologically Inspired Engineering, Harvard University

8 \* To whom correspondence should be addressed  
9

10 ABSTRACT

11 Bacteria from several taxa, including *Kurthia zopfii*, *Myxococcus xanthus*, and *Bacillus mycoides*, have  
12 been reported to align growth of their colonies to small features on the surface of solid media, including  
13 anisotropies created by compression. While the function of this phenomenon is unclear, it may help  
14 organisms navigate on solid phases, such as soil. The origin of this behavior is also unknown: it may be  
15 biological (that is, dependent on components that sense the environment and regulate growth  
16 accordingly) or merely physical.

17 Here we show that *B. subtilis*, an organism that typically does not respond to media compression, can be  
18 induced to do so with two simple and synergistic perturbations: a mutation that maintains cells in the  
19 swarming (chained) state, and the addition of EDTA to the growth media, which further increases chain  
20 length. EDTA apparently increases chain length by inducing defects in cell separation, as the treatment  
21 has only marginal effects on the length of individual cells.

22 These results lead us to three conclusions. First, the wealth of genetic tools available to *B. subtilis* will  
23 provide a new, tractable chassis for engineering compression sensitive organisms. Second, the  
24 sensitivity of colony morphology to media compression in *Bacillus* is a physical rather than biological  
25 phenomenon dependent on a simple physical property of rod-shaped cells. And third, colony  
26 morphology under compression holds promise as a rapid, simple, and low-cost way to screen for  
27 changes in the length of rod-shaped cells or chains thereof.

## 28 INTRODUCTION

29 Response of bacterial colony morphology (ie, orientation of growth) to small mechanical perturbations  
 30 of growth media was first noted in *Kurthia*, a gram-positive genus notable for its striking feather-like  
 31 morphology on gelatin slant cultures.(Sergent, 1906, 1907; Jacobsen, 1907; Stackebrandt, Keddie &  
 32 Jones, 2006) A similar compression response has been reported in *Myxococcus xanthus*, where the  
 33 phenomenon is dependent on adventurous motility, a flagellum- and pili-independent movement  
 34 system.(Stanier, 1942; Fontes & Kaiser, 1999; Nan et al., 2014) Recently, the soil bacterium *Bacillus*  
 35 *mycooides* was also shown to be sensitive to media perturbations.(Stratford, Woodley & Park, 2013)  
 36 Interestingly, this compression response seems to occur by two different mechanisms: whereas  
 37 individual *Myxococcus xanthus* dynamically reorients individual cells along lines of  
 38 compression,(Dworkin, 1983) *Bacillus mycooides* instead gradually reorients the tips of chained cells as it  
 39 grows.(Stratford et al., 2013)

40 The function of compression response is not known, but it has been suggested to aid navigation in  
 41 natural environments on solid phases, like soil.(Dworkin, 1983) It has also been proposed as a potential  
 42 tool for engineering applications in sensing environmental forces or generating patterns for  
 43 nanofabrication.(Stratford et al., 2013)

44 Here we investigate whether increasing the length of chains of cells can induce compression sensitivity  
 45 in an otherwise compression-insensitive species, *B. subtilis*. We employ a mutant of *B. subtilis* that forms  
 46 long chains of cells (much like *B. mycooides*) and also deplete divalent cations in the media with EDTA;  
 47  $Mg^{2+}$  is thought to be important for cell wall integrity. *B. subtilis* deprived of magnesium accumulates cell  
 48 wall precursors,(Garrett, 1969) and magnesium is known to bind to components of the cell  
 49 wall.(Heckels, Lambert & Baddiley, 1977) Notably, high magnesium concentrations can restore rod  
 50 shape to cells with mutations in MreB, MreD, and PonA – all genes involved in cell wall  
 51 synthesis.(Rogers, Thurman & Buxton, 1976; Rogers & Thurman, 1978; Murray, Popham & Setlow, 1998;  
 52 Formstone & Errington, 2005)

53

## 54 MATERIALS AND METHODS

### 55 Table 2. Strains used in this study

Designation	Description	Reference
<i>B. subtilis</i> PY79	Lab strain	Bacillus Genetic Stock Center 1A747
<i>B. subtilis</i> $\sigma^D::tet$	RL4169, DS323	Kearns and Losick, 2005 (Kearns & Losick, 2005)
<i>B. mycooides</i>		ATCC 6462

56

### 57 Time lapse microscopy

58 2% LB agar was cut into approximately 10mm x 10mm squares and inoculated with 1 $\mu$ l of liquid culture.  
 59 The pad was then wedged, in a glass-bottomed dish (P35G-1.5-20-C, MatTek Corp.), between two plastic  
 60 coverslips (Rinzi Plastic Coverslips, Size 22x22mm, Electron Microscopy Science) manually bent in half at  
 61 a 90° angle. Thus, half of each plastic coverslip made contact with the bottom of the dish, while the  
 62 other half made contact with the agar pad. After placing a drop of approximately 50 $\mu$ l of water on top of

63 each plastic coverslip to maintain humidity in the dish, the MatTek dish was sealed with parafilm (this  
64 setup is illustrated in Fig. 1A). Cells were grown for approximately 6 hours at room temperature  
65 (approximately 23°) during a timelapse acquisition on a Nikon TE 2000 microscope equipped with an  
66 Orca ER camera, a 20x phase contrast objective, and Perfect Focus. A large area of the sample was  
67 composited with automatic image stitching by Nikon Elements AR. Areas toward the center of the pad  
68 were selected for imaging.

#### 69 **Plate compression**

70 Microtiter format plates were prepared with LB + 2% agar. 24 hours after plates were poured, sterilized  
71 polystyrene spacers (each 0.080" thick, for a total compression of 0.16" or 4.1mm, equivalent to 4.8%  
72 compression) were inserted along the long dimension. Plates were stored at 37° for 24 hours, then  
73 inoculated from colonies grown on LB agar. Plates were incubated for 2-3 days at 30°, as the time  
74 required to reach colony dimensions >8mm varied with EDTA concentration. After incubation, plates  
75 were imaged with a gel imager and colony dimensions measured with FIJI.(Schindelin et al., 2012)

#### 76 **Cellular morphology**

77 Colonies were grown on LB + 2% agar containing either 0 or 125µM EDTA. After 24 hours of incubation  
78 at 30°, cells from the edges of colonies were transferred directly to LB + 2% agar pads for imaging with  
79 the rounded bottoms of 0.6µl centrifuge tubes. To each pad, 1µl of an aqueous solution containing  
80 10µg/ml FM4-64 (Invitrogen) was added. Cells were imaged with a 100X phase contrast objective, and  
81 cell and chain lengths were measured manually with spline-fitted segmented lines in FIJI. Two-sample KS  
82 tests were performed.(Kirkman, 1996)

83

## 84 **RESULTS**

85 We first noted weak compression response of *B. subtilis* under the microscope. Unlike *B. mycooides*, *B.*  
86 *subtilis* colonies remain circular under compression under normal conditions. However, our microscopy  
87 assay (Fig. 1A) revealed that at small length scales (<100µm), *B. subtilis* cells display short-range  
88 alignment perpendicular to the direction of compression (marked with black arrows in Fig. 1A-C). Noting  
89 that the alignment is disrupted over longer length scales, we sought conditions under which *B. subtilis*  
90 cells might behave more similarly to *B. mycooides*. We noted that the chains of *B. subtilis* PY79 appeared  
91 shorter than that of *B. mycooides*, with the former reaching a maximum of approximately 300µm (Fig.  
92 1C), while the can extend for millimeters(Stratford et al., 2013).

93 To increase chain length, we used *B. subtilis*  $\sigma^D::tet$ , a mutant that does not switch from swimming to  
94 swarming motility, and thus grows in long chains of cells (Kearns & Losick, 2005). To further perturb cell  
95 separation, we added EDTA to the growth medium.

96 To study colony morphology of *B. subtilis* under compression at the macroscopic scale with reproducible  
97 compression conditions, we prepared microtiter plates with LB + 2% agar and wedged polystyrene  
98 spacers between the agar and an edge of the plates (Fig. 2A). We inoculated the agar with colonies of *B.*  
99 *mycooides*, *B. subtilis* PY79, and *B. subtilis*  $\sigma^D::tet$ . Under 4.8% compression, *B. mycooides* forms elongated  
100 colonies as reported,(Stratford et al., 2013) while, without EDTA, *B. subtilis* colonies are round (Fig. 2A).  
101 With the addition of EDTA to the media, both *B. subtilis* PY79 and  $\sigma^D::tet$  display a compression response

102 (Fig. 2B). This is dependent on the degree of compression; at 2.4% compression, both *B. subtilis* strains  
103 formed round colonies (data not shown).

104 We next quantified this effect over several colonies under each EDTA condition at 4.8% compression.  
105 *Bacillus mycooides* forms colonies 4-4.5x larger in the dimension perpendicular to the direction of  
106 compression than parallel to it regardless of EDTA concentration (Fig. 2C). In comparison, the effect in *B.*  
107 *subtilis* is relatively small. *Bacillus subtilis* colonies were a maximum of approximately 1.5x larger in the  
108 direction perpendicular to compression, and this effect scaled with EDTA concentration (Fig. 2C). The  
109 EDTA effect was stronger for the  $\sigma^D::tet$  strain; at 125 $\mu$ M EDTA, compressed  $\sigma^D::tet$  colonies were 1.64x  
110 larger in the direction of compression (n=17, standard deviation 0.21), while PY79 colonies were 1.23x  
111 larger (n=16, standard deviation 0.20).

112 To understand how EDTA could affect compression response, we imaged cells taken directly from the  
113 edges of colonies on solid media containing either 0 $\mu$ M (Fig. 3A-C) or 125 $\mu$ M EDTA (Fig. 3D-F). The  
114 chains of *B. subtilis* cells, both PY79 and  $\sigma^D::tet$ , are longer on 125 $\mu$ M EDTA, but cell lengths, as  
115 delineated by the membrane dye FM4-64, are only marginally different. Quantification of ~300 chain  
116 and cell lengths for each strain under each condition (Fig. 4) reveals that *B. subtilis* chain lengths  
117 increase dramatically with the presence of EDTA, while *B. mycooides* chain lengths decrease slightly,  
118 suggesting that the EDTA effect on cell separation is specific to *B. subtilis* (Table 1).

119 **Table 1. Properties of cell and chain length measurement distributions**

	Cell length			Chain length		
	0 $\mu$ M EDTA mean ( $\mu$ m)	125 $\mu$ M EDTA mean ( $\mu$ m)	KS test maximum difference	0 $\mu$ M EDTA mean ( $\mu$ m)	125 $\mu$ M EDTA mean ( $\mu$ m)	KS test maximum difference
<i>B. mycooides</i>	4.01 (st dev 1.54)	4.33 (st dev 2.04)	D = 0.1044, P = 0.051	9.19 (st dev 4.81)	6.60 (st dev 3.09)	D = 0.2959, P = 0.000
<i>B. subtilis</i> PY79	3.18 (st dev 1.03)	4.18 (st dev 1.93)	D = 0.2866, P = 0.000	3.94 (st dev 1.38)	13.71 (st dev 7.23)	D = 0.8505, P = 0.000
<i>B. subtilis</i> $\sigma^D::tet$	4.23 (st dev 3.20)	4.12 (st dev 2.18)	D = 0.2413, P = 0.000	7.50 (st dev 3.36)	21.99 (st dev 18.1)	D = 0.5633, P = 0.000

120

## 121 DISCUSSION

122 These results suggest that the phenomenon of colony orientation under compression can be induced in  
123 the model organism *B. subtilis*. In contrast to *Bacillus mycooides*, the genetic tractability of *B. subtilis* will  
124 facilitate engineering of compression sensitive bacteria for use as environmental sensors or guides for  
125 nanofabrication.(Stratford et al., 2013)

126 Furthermore, the fact that that colony orientation on compressed media is generalizable indicates that it  
127 is likely to be a physical phenomenon. Rather than requiring biological components specific to *B.*  
128 *mycooides*, it is probably based on factors like rod length, stiffness, and tip vs. isotropic growth pattern.

129 Long rod length is a common feature of two prototypical compression responders, *Bacillus mycoides* and  
130 *Kurthia sp.*, which both grow as long chains of cells.(Di Franco et al., 2002; Stackebrandt et al., 2006) As  
131 seen in microscopy of *B. mycoides*, the absence of cell separation allows the bacteria to find and  
132 maintain a direction of compression. This same chaining property is responsible for the baroque colony  
133 morphology of *B. mycoides*: mutants that do not display this colony morphology have shorter chain  
134 lengths.(Di Franco et al., 2002) Thus, compression response may be driven by the same mechanisms that  
135 influence colony morphology under normal conditions; these mechanisms influence the manner in  
136 which cells explore and colonize their environment, and may be of critical importance in soil  
137 environments.

138 In the case of *B. subtilis*, the increase in compression sensitivity is based on chain length (as a  $\sigma^D$  mutant  
139 responds more than PY79, and both respond more strongly in the presence of EDTA, which also  
140 increases rod length). Though EDTA likely affects multiple cellular processes, the role of  $Mg^{2+}$  in cell wall  
141 formation is clear.(Formstone & Errington, 2005) In particular, peptidoglycan hydrolases called  
142 autolysins are implicated in separation of cells after septation. Some of these autolysins, such as LytC, D,  
143 and F, are under the control of  $\sigma^D$ .(Chen et al., 2009) However, LytC expression can also be driven by  
144  $\sigma^A$ .(Lazarevic et al., 1992) and this 50kDa amidase is activated by addition of  $Mg^{2+}$  *in vitro*.(Foster, 1992)  
145 This magnesium dependence of LytC and its regulation by a second sigma factor may explain why EDTA  
146 treatment further increases chain length in  $\sigma^D::tet$  cells. In addition to LytC, EDTA may be acting on other  
147 autolysins not regulated by  $\sigma^D$  (such as LytE or YwbG).(Smith, Blackman & Foster, 2000) The insensitivity  
148 of *B. mycoides* chain length to EDTA (Fig. 4, table 1) may be explained by species-specific differences in  
149 autolysins.

150 Inhibition of cell separation may not be the only relevant effect of EDTA, however. For example, perhaps  
151 depletion of  $Mg^{2+}$  changes the rigidity of cells such that they more readily align with the isotropic agar  
152 surface (Fig. 1B). An exhaustive understanding of EDTA's effects on the mechanical properties of *B.*  
153 *subtilis* walls remains to be attained.

154 The relatively weak maximal compression response we achieved with *B. subtilis* compared to *B.*  
155 *mycoides* suggests that other factors limit the compression response of *B. subtilis*. We suggest that one  
156 contributing factor is the growth pattern of this organism. Whereas *B. mycoides* elongates from its  
157 tips,(Turchi et al., 2012) *B. subtilis* inserts cell wall isotropically along its length.(Tiyanont et al., 2006) In  
158 micrographs of *B. subtilis* under compression, the chains of cells appear more buckled than those of *B.*  
159 *mycoides* (Fig. 1C); perhaps friction prevents the distal ends of the chain from sliding along to  
160 accommodate new growth from the middle of the chain. This buckling disrupts adjacent chains and is  
161 likely to lead to a more disorganized colony morphology. In the future, further modifications, perhaps  
162 increasing surfactin production, may increase the magnitude of this response.

163 Finally, because *B. subtilis* compression response depends on chain length, we propose that under some  
164 circumstances, colony morphology under compression could serve as a simple, high-throughput assay  
165 for perturbations to bacterial cell length and chain formation.

166  
167  
168  
169  
170  
171  
172  
173  
174  
175  
176  
177  
178  
179  
180  
181  
182  
183  
184  
185  
186  
187  
188  
189  
190  
191

## ACKNOWLEDGEMENTS

We thank Ethan Garner (Harvard University), Michael Baym (Harvard Medical School) and Ariel Amir (Harvard University) for helpful discussions. We are grateful to Stephanie Hays (Harvard Medical School) for critical reading of the manuscript.

## REFERENCES

- Chen R, Guttenplan SB, Blair KM, Kearns DB. 2009. Role of the  $\sigma$ D-Dependent Autolysins in *Bacillus subtilis* Population Heterogeneity. *Journal of Bacteriology* 191:5775–5784.
- Dworkin M. 1983. Tactic behavior of *Myxococcus xanthus*. *Journal of Bacteriology* 154:452–459.
- Fontes M, Kaiser D. 1999. *Myxococcus* cells respond to elastic forces in their substrate. *Proceedings of the National Academy of Sciences* 96:8052–8057.
- Formstone A, Errington J. 2005. A magnesium-dependent *mreB* null mutant: implications for the role of *mreB* in *Bacillus subtilis*. *Molecular Microbiology* 55:1646–1657.
- Foster SJ. 1992. Analysis of the autolysins of *Bacillus subtilis* 168 during vegetative growth and differentiation by using renaturing polyacrylamide gel electrophoresis. *Journal of Bacteriology* 174:464–470.
- Di Franco C, Beccari E, Santini T, Pisaneschi G, Tecce G. 2002. Colony shape as a genetic trait in the pattern-forming *Bacillus mycoides*. *BMC Microbiology* 2:33.
- Garrett AJ. 1969. The effect of magnesium ion deprivation on the synthesis of mucopeptide and its precursors in *Bacillus subtilis*. *The Biochemical Journal* 115:419–430.
- Heckels JE, Lambert PA, Baddiley J. 1977. Binding of magnesium ions to cell walls of *Bacillus subtilis* W23 containing teichoic acid or teichuronic acid. *Biochemical Journal* 162:359–365.
- Jacobsen H. 1907. Ueber einen richtenden Einfluss beim Wachstum gewisser Bakterien in Gelatine. *Zentr. Bakt. Parasitenk.* II:53–64.

192 Kearns DB, Losick R. 2005. Cell population heterogeneity during growth of *Bacillus subtilis*. *Genes &*  
193 *Development* 19:3083–3094.

194 Kirkman T. 1996. Statistics to use.

195 Lazarevic V, Margot P, Soldo B, Karamata D. 1992. Sequencing and analysis of the *Bacillus subtilis*  
196 *lytRABC* divergon: A regulatory unit encompassing the structural genes of the N-  
197 acetylmuramoyl-L-alanine amidase and its modifier. *Journal of General Microbiology* 138:1949–  
198 1961.

199 Murray T, Popham DL, Setlow P. 1998. *Bacillus subtilis* cells lacking penicillin-binding protein 1 require  
200 increased levels of divalent cations for growth. *Journal of Bacteriology* 180:4555–4563.

201 Nan B, McBride MJ, Chen J, Zusman DR, Oster G. 2014. Bacteria that Glide with Helical Tracks. *Current*  
202 *Biology* 24:R169–R173.

203 Rogers HJ, Thurman PF. 1978. Temperature-sensitive nature of the *rodB* maturation in *Bacillus subtilis*.  
204 *Journal of Bacteriology* 133:298–305.

205 Rogers HJ, Thurman PF, Buxton RS. 1976. Magnesium and anion requirements of *rodB* mutants of  
206 *Bacillus subtilis*. *Journal of Bacteriology* 125:556–564.

207 Schindelin J, Arganda-Carreras I, Frise E, Kaynig V, Longair M, Pietzsch T, Preibisch S, Rueden C, Saalfeld  
208 S, Schmid B et al. 2012. Fiji: an open-source platform for biological-image analysis. *Nature*  
209 *Methods* 9:676–682.

210 Sergent E. 1906. Des tropismes du “*Bacterium zopfii*” Kurth. Premiere note. *Ann. inst. Pasteur*:1005–  
211 1017.

212 Sergent E. 1907. Des tropismes du “*Bacterium zopfii*” Kurth. Deuxieme note. *Ann. inst. Pasteur*:842–850.

213 Smith TJ, Blackman SA, Foster SJ. 2000. Autolysins of *Bacillus subtilis*: multiple enzymes with multiple  
214 functions. *Microbiology* 146:249–262.



215 Stackebrandt E, Keddie RM, Jones D. 2006. The Genus Kurthia. In: Dr MDP, Falkow S, Rosenberg E,  
216 Schleifer K-H, Stackebrandt E eds. *The Prokaryotes*. Springer US, 519–529.

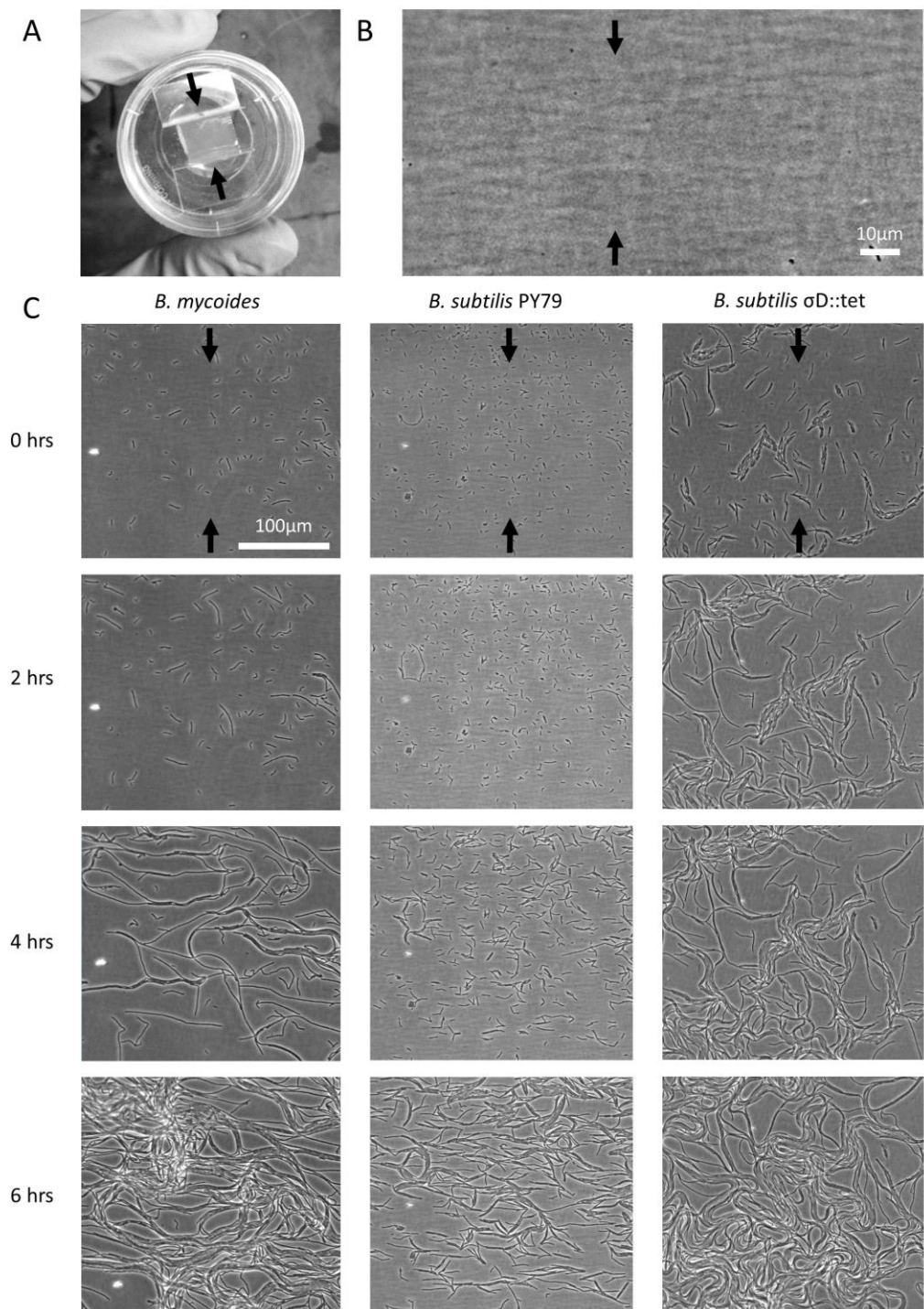
217 Stanier RY. 1942. A Note on Elasticotaxis in Myxobacteria. *Journal of Bacteriology* 44:405–412.

218 Stratford JP, Woodley MA, Park S. 2013. Variation in the Morphology of *Bacillus mycoides* Due to  
219 Applied Force and Substrate Structure. *PLoS ONE* 8:e81549.

220 Tiyanont K, Doan T, Lazarus MB, Fang X, Rudner DZ, Walker S. 2006. Imaging peptidoglycan biosynthesis  
221 in *Bacillus subtilis* with fluorescent antibiotics. *Proceedings of the National Academy of Sciences*  
222 *of the United States of America* 103:11033–11038.

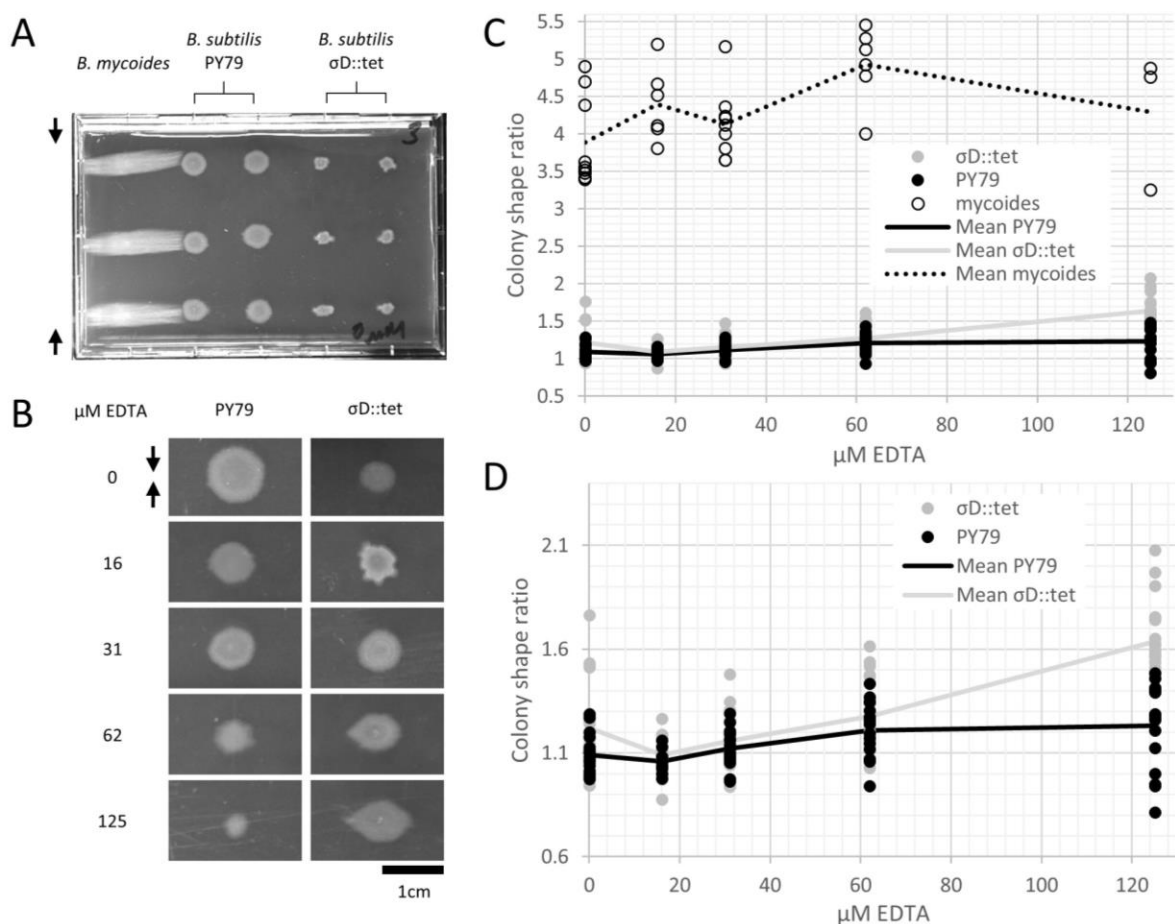
223 Turchi L, Santini T, Beccari E, Di Franco C. 2012. Localization of new peptidoglycan at poles in *Bacillus*  
224 *mycoides*, a member of the *Bacillus cereus* group. *Archives of Microbiology* 194:887–892.

225  
226



227

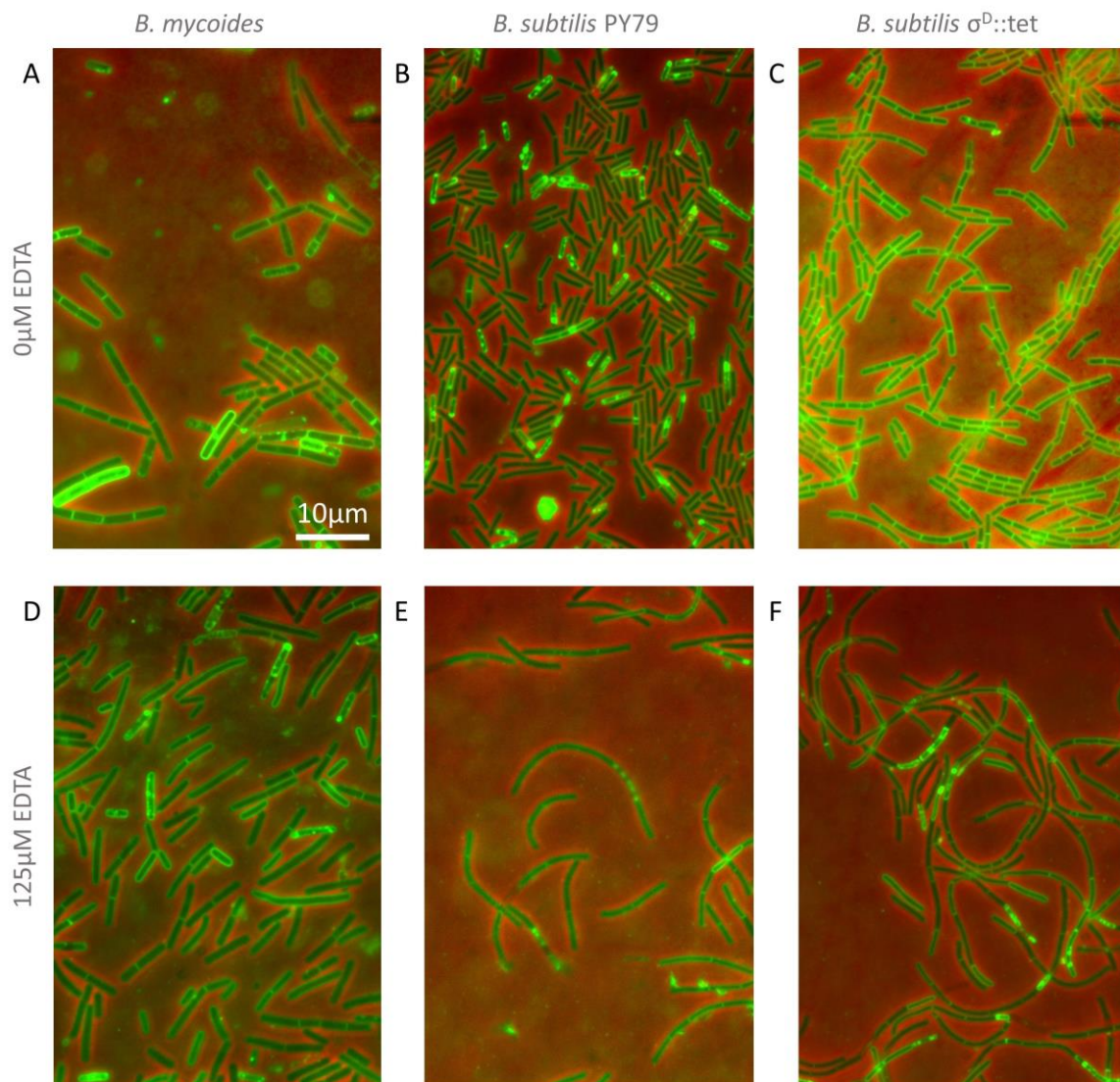
228 **Figure 1. Microscopic morphology of *B. mycooides* and *B. subtilis* under compression.** A) Cells from  
 229 liquid culture were applied to the bottom of an agarose pad compressed between plastic coverslips in a  
 230 MatTek dish. Black arrows indicate direction of compression throughout. B) Striations visible in agar  
 231 surfaces. C) Montages of timelapses of *B. mycooides*, *B. subtilis* PY79, and *B. subtilis*  $\sigma^D::tet$ . Note the  
 232 striations visible in the agarose running perpendicular to the direction of compression.



233

234 **Figure 2. *B. mycooides* and *B. subtilis* colony morphology under compression.** A) A microtiter plate  
 235 inoculated with *B. mycooides* and *B. subtilis*. The two white bars at the top of the image of the plate are  
 236 polystyrene spacers, totaling 4.8% of the plate height. Black arrows indicate direction of compression  
 237 throughout. B) Representative images of *B. subtilis* PY79 and  $\sigma$ D::tet colonies grown on compressed agar  
 238 with varying EDTA concentrations. Scale bar, 1cm. C) Plot of colony shape ratio (ie, colony measurement  
 239 perpendicular to the dimension of compression/colony measurement parallel to the dimension of  
 240 compression) as it varies with EDTA concentration. D) Same as in C but with axes scaled to emphasize  
 241 relative effect of PY79 and  $\sigma$ D::tet.

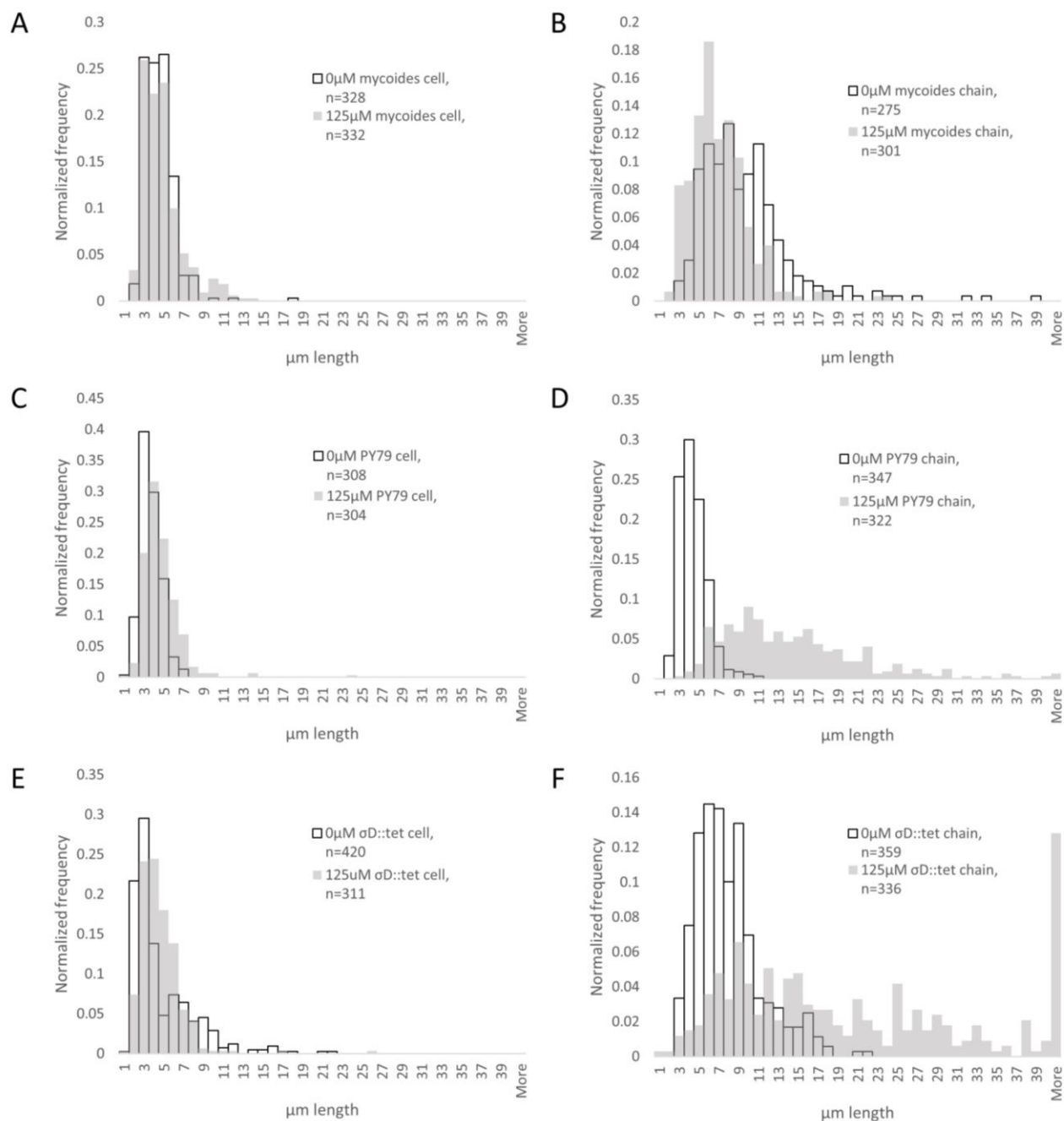
242



243

244 **Figure 3. Cellular morphology with and without EDTA.** A-C) *B. mycooides*, *B. subtilis* PY79, and *B. subtilis*  
245  $\sigma^D::tet$ , respectively, growing on LB agar containing 0  $\mu$ M EDTA. D-F) As above on 125  $\mu$ M EDTA. In all  
246 images, phase contrast channel is in red, and FM4-64 is in green. Scale bar, 10  $\mu$ m.

247



248

249 **Figure 4. Quantification of chain and cell lengths with and without EDTA.** A) Cell lengths of *B. mycoides*  
 250 on 0 μM (hollow bars) and 125 μM EDTA (grey bars). B) Chain lengths of *B. mycoides*. C) Cell lengths of *B.*  
 251 *subtilis* PY79. D) Chain lengths of *B. subtilis* PY79. E) Cell lengths of *B. subtilis* σD::tet. F) Chain lengths of  
 252 *B. subtilis* σD::tet.